




Article

Modification of Poly(vinylidene fluoride-co-hexafluoropropylene) Membranes with DES-Functionalized Carbon Nanospheres for Removal of Methyl Orange by Membrane Distillation

Mustafa Mohammed Aljumaily ¹, Nisreen S. Ali ², Alyaa Esam Mahdi ³, Haiyam M. Alayan ³, Mohamed AlOmar ¹ , Mohammed Majeed Hameed ^{1,4} , Bashar Ismael ¹, Qusay F. Alsalhy ^{3,*}, Mohammed A. Alsaadi ⁵ , Hasan Sh. Majdi ⁶ and Zainab Bahaa Mohammed ⁷

- ¹ Department of Civil Engineering, Al-Maaref University College, Ramadi 31001, Iraq; mustafa.k@uoa.edu.iq (M.M.A.); mohd.alomar@yahoo.com (M.A.); m.majeed@uoa.edu.iq (M.M.H.); bashar.h.ismael@uoa.edu.iq (B.I.)
- ² Materials Engineering Department, College of Engineering, Al-Mustansiriyah University, Baghdad 14022, Iraq; nisreensabah@uomustansiriyah.edu.iq
- ³ Membrane Technology Research Unit, Chemical Engineering Department, University of Technology-Iraq, Alsenaa Street 52, Baghdad 10066, Iraq; alyaa.e.mahdi@uotechnology.edu.iq (A.E.M.); haiyam.m.abdalraheem@uotechnology.edu.iq (H.M.A.)
- ⁴ Department of Civil Engineering, Faculty of Engineering and Built Environment, Universiti Kebangsaan Malaysia, Bangi 43600, Selangor, Malaysia
- ⁵ National Chair of Materials Science and Metallurgy, University of Nizwa, Nizwa 611, Oman; m.hakim@unizwa.edu.om
- ⁶ Department of Chemical Engineering and Petroleum Industries, Al-Mustaqbal University College, Babylon 51001, Iraq; dr.hasanshker@mustaqbal-college.edu.iq
- ⁷ Department of Civil Engineering, University of Technology-Iraq, Alsenaa Street 52, Baghdad 10066, Iraq; 40188@uotechnology.edu.iq
- * Correspondence: qusay.f.abdulhameed@uotechnology.edu.iq or qusay_alsalhy@yahoo.com



Citation: Aljumaily, M.M.; Ali, N.S.; Mahdi, A.E.; Alayan, H.M.; AlOmar, M.; Hameed, M.M.; Ismael, B.; Alsalhy, Q.F.; Alsaadi, M.A.; Majdi, H.S.; et al. Modification of Poly(vinylidene fluoride-co-hexafluoropropylene) Membranes with DES-Functionalized Carbon Nanospheres for Removal of Methyl Orange by Membrane Distillation. *Water* **2022**, *14*, 1396. <https://doi.org/10.3390/w14091396>

Academic Editors: Zhe Yang and Peng-Fei Sun

Received: 24 March 2022

Accepted: 23 April 2022

Published: 26 April 2022

Publisher's Note: MDPI stays neutral with regard to jurisdictional claims in published maps and institutional affiliations.



Copyright: © 2022 by the authors. Licensee MDPI, Basel, Switzerland. This article is an open access article distributed under the terms and conditions of the Creative Commons Attribution (CC BY) license (<https://creativecommons.org/licenses/by/4.0/>).

Abstract: Chemical pollutants, such as methyl orange (MO), constitute the main ingredients in the textile industry wastewater, and specifically, the dyeing process. The use of such chemicals leads to huge quantities of unfixed dyes to make their way to the water effluent and consequently escalates the water pollution problem. This work investigates the incorporation of hydrophobic carbon nanospheres (CNS) prepared from the pyrolysis of acetylene using the chemical vapor deposition technique with poly(vinylidene fluoride-co-hexafluoropropylene) (PVDF-HFP) in order to enhance its hydrophobicity. Moreover, a deep eutectic solvent (DES) was used to enhance the membrane's porosity. The former was based on the quaternary ammonium salt (N,N-diethyl-ethanol-ammonium chloride) as a chemical addition throughout the membrane synthesis. Direct contact membrane distillation (DCMD) was employed to assess the performance of the modified membrane for treatment of MO contaminated water. The phase inversion method was used to embed various contents of CNS (i.e., 1.0, 3.0, and 5.0 wt.%) with 22:78 wt.% of PVDF-co-HFP/N-Methyl-2-pyrrolidone solution to prepare flat-sheet membranes. The membrane embedded with 5 wt.% CNS resulted in an increase in membrane hydrophobicity and presented considerable enhancement in DCMD permeation from 12 to 35 L/h.m² with salt rejection >99.9%. Moreover, the composite membrane showed excellent anti-biofouling and mechanical characteristics as compared to the pristine counterpart. Using this membrane, a complete rejection of MO was achieved due to the synergistic contribution of the dye negative charge and the size exclusion effect.

Keywords: PVDF-HFP; membrane distillation; deep eutectic solvent; methyl orange; wastewater treatment; anti-biofouling

1. Introduction

The reuse of wastewater using advanced treatment technologies is considered as an emerging solution to satisfy our demands and to alleviate the deficiency of potential sources of clean water [1]. The reuse of water and wastewater using advanced treatment technologies to fulfill both national and industrial necessities is considered as one of the crucial keys to face the deficiency of potential sources of clean water [2]. The large release of wastewaters containing different species of dyes is ecologically dangerous to individuals and the environment [3]. The wastewaters' massive unloading, which includes various types of dyes, poses a serious threat to the environment and endangers human health [4]. Purification of dye wastewaters resulting from the textile industry has been introduced as one of the effective approaches to deal with water scarcity [5].

Methyl orange (MO) has an aromatic structure and degrades to carcinogenic products, which makes them tougher to clean. Hence, the removal of MO dye from wastewater can be achieved through the use of various physicochemical methods [6]. However, the implementation of these methods has inherent shortcomings, such as inefficiency for dilute solutions, by-product sludge, and the demand for high-level treatment. MO is an illustration of toxic anionic and biologically nondegradable azo dye. It is difficult to remove MO due to its aromatic structure, which degrades to mutagenic or carcinogenic products [7]. As a result, some methods were used to treat wastewaters containing the MO dye, namely biodegradation, extraction, electrophoresis, coagulation, photocatalysis, oxidation, and adsorption [8,9]. Nonetheless, it is worth mentioning that the previously stated techniques hold some disadvantages, such as inefficiency for dilute solutions, by-product sludge, and the need for post-treatment.

Membrane separation techniques have been widely employed as highly reliable technologies in water and wastewaters treatment. Therefore, there is an eager need to improve the physio-chemical properties and membranes' permeability [10,11]. Hierarchical or hybrid matrix membranes fabricated through the integration of particular materials which have unique features in their structures offer the most attractive types of membranes. Hierarchical or mixed matrix membranes produced by means of incorporating some specialized materials with unique individualities into their structures represent one of the most attractive types of membranes [12]. Since the main separation mechanisms in these membranes occur due to sieving, charge interactions, and/or solute-membrane selectivity, the inclusion of CNSs into the membrane matrix has shown an enhancement in the membrane structure and improved its perm-affinity [13]. Charge repulsion and/or solute-membrane affinity and size exclusion are the central parting techniques in these membranes.

The method of membrane distillation (MD) operates due to the vapor pressure gradient, which is mostly controlled by the heated feed across a hydrophobic membrane. The membrane works as a border amidst the hot seawater feed and the permeated vapor condensed using the direct contact membrane distillation (DCMD). The vapor partial pressure, which goes across a hydrophobic membrane, is responsible for operating the thermally driven method of membrane distillation (MD) [14]. The hydrophobic membrane acts as a boundary in the midst of the hot seawater feed and the cold freshwater permeate that straightforwardly interacts with the membrane distillation (DCMD) [15]. The hydrophobicity effect of the membrane permits the passage of water vapor merely within the micro-pores by the water vapor partial pressure driving force [16]. Compared to other polymers, the poly(vinylidene fluoride-hexafluoropropylene) (PVDF-HFP) has attracted attention as a potential polymeric membrane for MD applications due to the developed amorphous phase content that leads to better hydrophobic chains and the confinement of various nanomaterials topography and topology ropes [17]. In the past few years, the exploitation of the formation of spherically shaped carbon nanospheres (CNS) has become topical and the literature is not very prolific [18]. While carbon nanotubes (CNTs) have been widely investigated, still very little research has been carried out using CNSs. CNSs are presently applied as catalyst support, lubricants, electronic devices, and wear-resistant materials, but their applications are immature. While carrying out extensive experimental

activity concerning polymer-carbon nanotubes composite, a new light has been cast on the possible use of CNSs for preparing a new generation of composites using CNSs instead of CNTs. It is worth mentioning that chemical vapor deposition (CVD) synthesized CNSs. This approach satisfies the requirements for continuously high yield production and provides purer CNSs even in the absence of a catalyst. This approach satisfies the requirements for the continuous production of high yield and pure CNSs even in the absence of a catalyst. CNSs have an integrated and intact structure with excellent versatile properties and high thermal stabilities [19]. Different substrates have been used in CVD on which hydrophobic CNS are typically grown. However, these substrates might cause an aggregation of CNS and often contain impurities, which need further cleaning and purification processes [20]. As a result, this will adversely affect the surface of the nanostructures and significantly decrease CA and it will have an unfavorable impact on the surface and dramatically reduce CA. So, the introduction of powder activated carbon (PAC) as a support was found worthy to be exploited. Additionally, to further enhance the rejection of the negatively charged methyl orange dye (MO), the prepared CNSs were functionalized. However, the modification of CNSs requires the utilization of harsh agents, which reshape surface, not to mention also causing a significant risk to the environment. Thus, it is crucial to incorporate green and cost-effective functionalization agents. Nevertheless, the functionalization of CNSs necessitates the employment of resilient acids and damaging agents that alter the morphology of the CNSs and also significantly endangers the environment.

Deep eutectic solvents (DESs) have enjoyed increasing popularity for the preceding decade as a promising replacement of conventional solvents and have shown remarkable compatibility with the common ionic liquids. The development of green solvents has attracted great concern in chemistry; thus, studies on DESs have been prosperous for the past decade and they are broadly recognized as a striking analog to the conventional ionic liquids (ILs) [21,22]. At first, Abbott et al. considered DESs to be a new associated group of ILs which are seamlessly known for their employment in various applications. The synthesis of DESs with tunable physical features is achieved through the combination of a quaternary ammonium compound with a hydrogen bond donor or a metal chloride in numerous molar ratios. DESs exhibit similar features to ILs and additional benefits, such as their quick, cheap, and facile way of preparation. Moreover, DES was first introduced by Abbott et al. as an inexpensive substitute to other ILs. The complexation of metal salt, which performs as a hydrogen bond donor with a quaternary ammonium salt, is the means of forming DESs, which have been applied lately in multiple scientific arenas [23,24]. Among the perks that they enjoy over other ionic liquids are their ease and low-cost synthesis and tunable physical features by variation of molar ratios of reactants [21,25]. However, to our knowledge, efficient water treatment using mixed matrix membranes containing functionalized carbon nanospheres have not been investigated in the literature.

For the sake of obtaining hydrophobic CNSs to scale-up the membrane fabrication, the current work used a CNS which has been prepared from the deposition of pyrolyzed acetylene on powdered activated carbon using the chemical vapor deposition method (CVD) [26]. The hybrid CNS/PAC enlightens a promising class of hybrids by directly growing carbon on micro-scaled carbon support. The fabricated CNS/PAC is chemically homogeneous as it consists basically of carbon, but poses a heterogeneous structure of different shapes. The produced hierarchical CNS was modified using *N,N*-diethyl-ethanol-ammonium chloride based DES and was incorporated in the polymer matrix to fabricate a CNS-DAC/PAC-PVDF-HFP composite membrane that was tested in our own designed DCMD setup for simultaneous salt and MO rejection.

2. Materials and Methods

2.1. Chemicals and Reagents

Nickel (II) nitrate hexahydrate, powder activated carbon (PAC), and methyl orange ($C_{14}H_{14}N_3NaO_3S$, MW = 327.34) were obtained from Sigma-Aldrich, Malaysia. Acetylene (C_2H_2), H_2 , and N_2 of purity 99.9% were bought from Malaysian Gas agency. The salt and

hydrogen bond donor (HBD) used for DES synthesis, i.e., N,N-diethylethanolammonium chloride (DAC) and ethylene glycol (EG), respectively, were both purchased from Merck. The membrane material, PVDF-HFP and N-Methyl-2-pyrrolidone solvent (NMP, >99.5%) were purchased from Sigma-Aldrich.

2.2. CNS Synthesis and Membrane Fabrication

2.2.1. Catalyst Impregnation

In total, 1 wt.% of nickel (II)-acetone solution was prepared in 5 mL and mixed with 2 g of PAC using sonication at 50 °C and 40 KHz until the acetone evaporated. The Ni doped PAC was dried overnight at 75 °C. The dried sample was carefully grinded, and the powder (i.e., Ni doped PAC) was stored in a desiccator.

2.2.2. Growth of CNS Using CVD

The placement of Ni doped PAC onto a ceramic in the middle of the CVD quartz tube was the means to synthesize the CNS-PAC superstructure. Calcination was performed by programming a temperature of 350 °C for 2 h under passive atmosphere (N₂, 200 mL/min), then a decrease to 450 °C under (H₂, 150 mL/min). At 750 °C C₂H₂ was mixed with H₂ at a ratio of 1-1 and the mixture was passed throughout the reaction tube for 40 min. After the CNSs progress, the reactor was cooled using N₂ flow (200 mL/min) and the CNSs were gathered from the ceramic boat. A KRUS Goniometer (DSA100) was used for CA measurements of the product.

2.3. Preparation of DES

Initial screening was performed to figure out the optimized molar ratio to fabricate uniform and stable DES. For the sake of minimizing the moisture content, DAC and EG were dried in a vacuum for 3 h. The used DES [DAC:EG] was synthesized by uniting DAC (salt) with EG (HBD) at [1:3] molar ratio. Salt and HBD were combined at 180 rpm and a temperature of 70 °C, which lasted for 80 min whilst awaiting the formation of a homogeneous transparent liquid. The prepared DES was stored in a moisture controlled environment for further functionalization use.

2.4. Functionalization of CNSs/PAC

Specifically, the 200 gm CNS sample was sonicated independently with 7 mL of DES for 3 h at 60 °C to produce DES functionalized nanostructure (DAC-CNS) followed by washing relying on a vacuum filtration system and drying under a vacuum for 24 h at 100 °C.

2.5. Preparation of Membranes

A phase inversion method has been employed in order to synthesize the blank PVDF-HFP/NMP membranes [27]. About 22:78 (wt.%/wt.%) polymer to solvent ratio was used. A magnetic stirrer at 400 rpm was used overnight to assure homogeneity of the mixture. Various concentrations of DES functionalized carbon nanospheres (DAC-CNSs: 1.0, 3.0, and 5.0 wt.%) were added to the mixture. A well-dispersed mixture of DAC-CNSs within the polymeric solution was obtained using an ultrasound bath for about 30 min. The prepared polymer solution was cast (the slot depth at 250 µm) into a thin film on a clean glass plate fixed on the casting machine at room temperature and then exposed to air for 30–60 s. The thin film was immersed into distilled water together with the glass plate until a wet film floated up to the water surface. The membrane was rinsed again with fresh distilled water for 24 h to complete the removal of the solvent's residues and dried at room temperature before further use.

2.6. Characterizations

The surface morphologies and topologies of the CNSs were examined through a transmission electron microscopy (TEM) (Hitachi-HT7700, 120 kV, Japan). A field-emission

scanning electron microscope (FE-SEM) (XL30 FEG, FEI Company) was employed to image the cross-section and surface morphologies of the composite membranes. Dried composite membrane samples were fragmented in liquid nitrogen and then sputtered with a thin layer of platinum utilizing SPI-Module sputter coater. Atomic force microscopy was used to test the composite membranes' surface roughness. The tensile strength test measurement at room temperature of the composite membranes was measured with an Instron 5940 tensile test machine. All samples were clamped at both ends of the machine and pulled in tension at an elongation velocity of 30 mm/min with an initial gauge length of 20 mm, and five samples were measured for each of the composite membranes and the average was calculated to get the results. The porosity void of the membranes ε_m (%) was obtained based on the density measurements compared with the membrane fabricated [28] following Equation (1):

$$\varepsilon_m (\%) = \left(1 - \frac{\rho_{cm}}{\rho_{control}} \right) \times 100 \quad (1)$$

where ρ_{cm} and $\rho_{control}$ are the densities of the membrane's composites and the PVDF-HFP, respectively. The density of PVDF-HFP has a value of 1.78 gm/cm³ according to the Sigma-Aldrich report.

2.7. Separation Performance Membranes

For the DCMD performance test, the membranes were placed inside a sealed polymer/DAC-CNS module. The DCMD unit consists of two spaces: one for deionized water and the other for polluted water separated by a double steel stile holding the DAC-CNS composite membrane, as shown in Figure 1. The composite membrane contact area was formed in a disc shape of 10.4 mm diameter. Two peristaltic pumps were employed in order to dominate both feed and permeate side streams, which were pumped in recirculation mode through heat and cool streams exchangers, respectively.

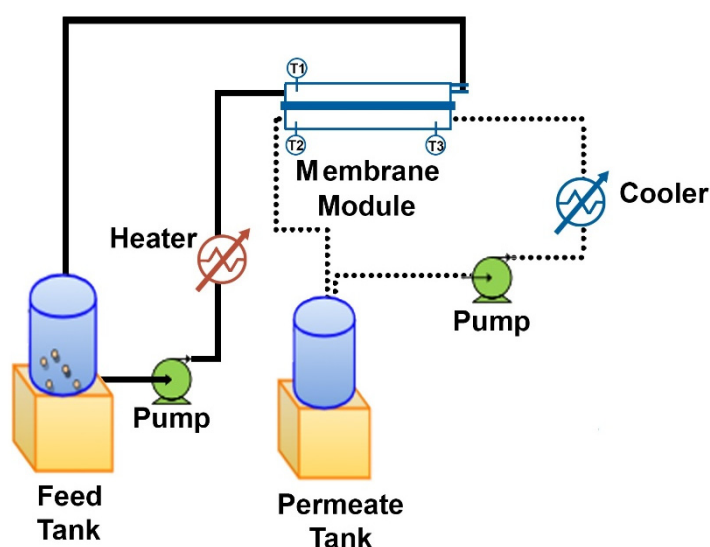


Figure 1. Process scheme of the DCMD setup.

Dissolving a dye powder in distilled water in order to make dye solutions, the determination of feed and permeate concentration was achieved through the usage of conductivity and total dissolved solid. The system was operated for 60 min with a feed flow rate of 22 mL/min and a permeate side stream flow rate of 12 mL/min [29].

Two thermocouples were used to constantly observe and preserve the DCMD's temperature on both sides: at 45 °C (feed side) and 20 °C (permeate side). The water volume moved to a permeate side as well as the electrical conductivity of the feed and perme-

ate side, which was monitored over time. The salt refusal, R%, was determined from Equation (2):

$$R(\%) = \left[1 - \left(C_p / C_f \right) \right] \times 100 \quad (2)$$

Taking into consideration that C_p is the permeate concentration and C_f is the feed concentration.

The assessment of cell performance was achieved through an identical token employing 50 mg/L of MO solution. The concentrations of numerous dyes before and after separation were evaluated using a UV-spectrophotometer (model Beckman DU640) at a maximum wavelength of 464 nm.

2.8. Antibacterial Testing

The chronic issue of membrane fouling, and specifically biofouling, delays the practical implementation of these membranes in separation applications. The CNS samples' biofouling activity against *Staphylococcus aureus* (*S. aureus*) 749 has been tested in order to reveal the viable-cell counting as described in the literature [30]. Initially, a nutrient broth was used to culture *S. aureus*, in order to get a stock with about 1.0×10^8 cells/mL. Next, 2 cm in diameter arranged samples have been exposed to the *S. aureus* cell suspension (100 mL containing about 4.86×10^8 cfu/mL). Amid a suitable dilution of *S. aureus* with sterilized 0.95% saline water, the sample was shaken at 250 rpm overnight at 37 °C. Afterwards, it was time for harvesting through a centrifugation at 3500 rpm for 30 min. Evaluation of the interaction of the PVDF-HFP and CNSs with *S. aureus* by SEM observation of *S. aureus* cells attached to the CNSs surface with a cell culture of the *S. aureus* (ca. 10^5 cfu/mL). The incubation of membranes lasted overnight on nutrient agar plates after 10 min immersion into the diluted *S. aureus* solution. Then, SEM was applied to observe the colony-forming units (CFUs) found on the membrane surface. The dipping of membranes into the diluted *S. aureus* solution was only for about 10 min before they were positioned and incubated on nutrient agar plates overnight. Lastly, SEM has been utilized to observe the colony-forming units (CFUs) on the membrane surface.

3. Results and Discussion

3.1. Synthesis CNSs

The effectively impregnated catalyst in the PAC has been visibly displayed in the transmission electron microscope (TEM) image (Figure 2a). Figure 2b shows graphitized uniform size ball-like beads (CNS) produced in the collected deposit. The carbon spheres attained frequently accumulate or bond together intending the formation of necklace chain-like structures. Moreover, an energy dispersive X-ray analysis (EDX) was relied on to carry out a deeper examination, as revealed in Figure 2c, which approved the PAC's inclusion of carbon (97 wt.%), oxygen (2 wt.%), and Ni (0.1 wt.%). This observation indicates that a small amount of Ni was adequate to promote the formation of catalytic sites on CNS.

3.2. Membrane Characterization

3.2.1. FT-IR Analysis

Fourier transform infrared spectroscopy was utilized to analyze the composite membranes' functional groups and PVDF-HFP. As can be seen in Figure 3, the spectrum of CNS revealed a different variety of functional groups. The dominant peaks at 1442, 1445, and 1552 cm^{-1} were exposed owing to stretching vibrations rings and peaks at wave numbers 1660 cm^{-1} , which is allied with C=O. Furthermore, two peaks were observed at 2926 and 2960 cm^{-1} , which are parallel to C-H stretching for sp^3 and sp^2 bonded carbon atom, respectively. Overall, it is worth mentioning that the contamination of CNS occurs on metal catalysts and it is covered by a graphitic nature shell, which is known by its oxidization when exposed to air in order to create few functional groups.

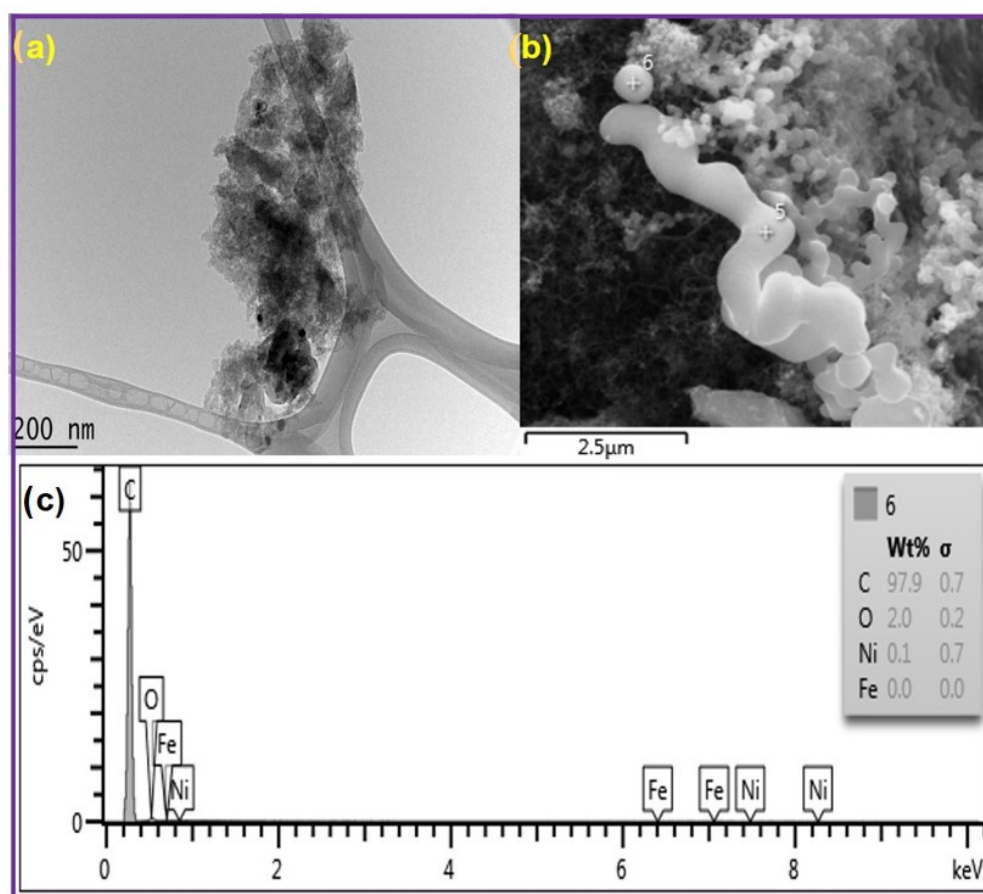


Figure 2. SEM and TEM images (a,b) for CNSs; (c) EDX analysis for PAC substrate.

Evidently, it is noteworthy that the CNS' spectrum has been considerably altered following the treatment with DES that confirms the capability of the functionalization process by the addition of new functional groups onto the CNSs' surface. The strong O–H stretching bond strong is assigned at $\sim 3460\text{ cm}^{-1}$. However, the N–H stretching bond could interfere with O–H in the zone of $(3500\text{--}3000)\text{ cm}^{-1}$. The C–H stretching bond is designated at $\sim 3750\text{ cm}^{-1}$ after functionalization. Additionally, regular and irregular stretching CH₂ groups are well-identified at $\sim 2900\text{ cm}^{-1}$ and $\sim 2800\text{ cm}^{-1}$, respectively [31]. The strong absorbance peak at $\sim 3460\text{ cm}^{-1}$ is allocated to the stretching bond O–H (hydroxyl groups) [32]. Nevertheless, in the area of $(3500\text{--}3000)\text{ cm}^{-1}$, an overlap of O–H may occur with N–H stretching bond [33]. The C–H stretching bond can be related to the rise of peaks at $\sim 3750\text{ cm}^{-1}$ after functionalization. Furthermore, a noticeable peak for about 2350 cm^{-1} is associated with aromatic sp^2 C–H stretching vibration [34]. In addition, the existence of peaks at ~ 1400 and $\sim 1650\text{ cm}^{-1}$ mirrors the creation of carbonyl groups and carboxylic acids onto CNSs after functionalization [35,36], while peaks in the area between $(800\text{--}600)\text{ cm}^{-1}$ are known to be related to C–Cl bond of the DES solvent [37]. A peak at 1660 cm^{-1} related to CNS-DAC membrane can be clearly distinguished from the spectrum, which is due to C=O stretching vibrations. These findings indicate that the CNSs were successfully grafted to the PVDF-HFP material. A minor prevalence of a crystalline stage is perceived in the PVDF-HFP membrane, as specified through the transmission peaks' existence at 528, 614, 760, 795, 840, 876, and 973 cm^{-1} . However, 974, 1070, 1180, 1280, and 1400 cm^{-1} are also observed and are ascribed to the polymer/solvent NMP interactions [8].

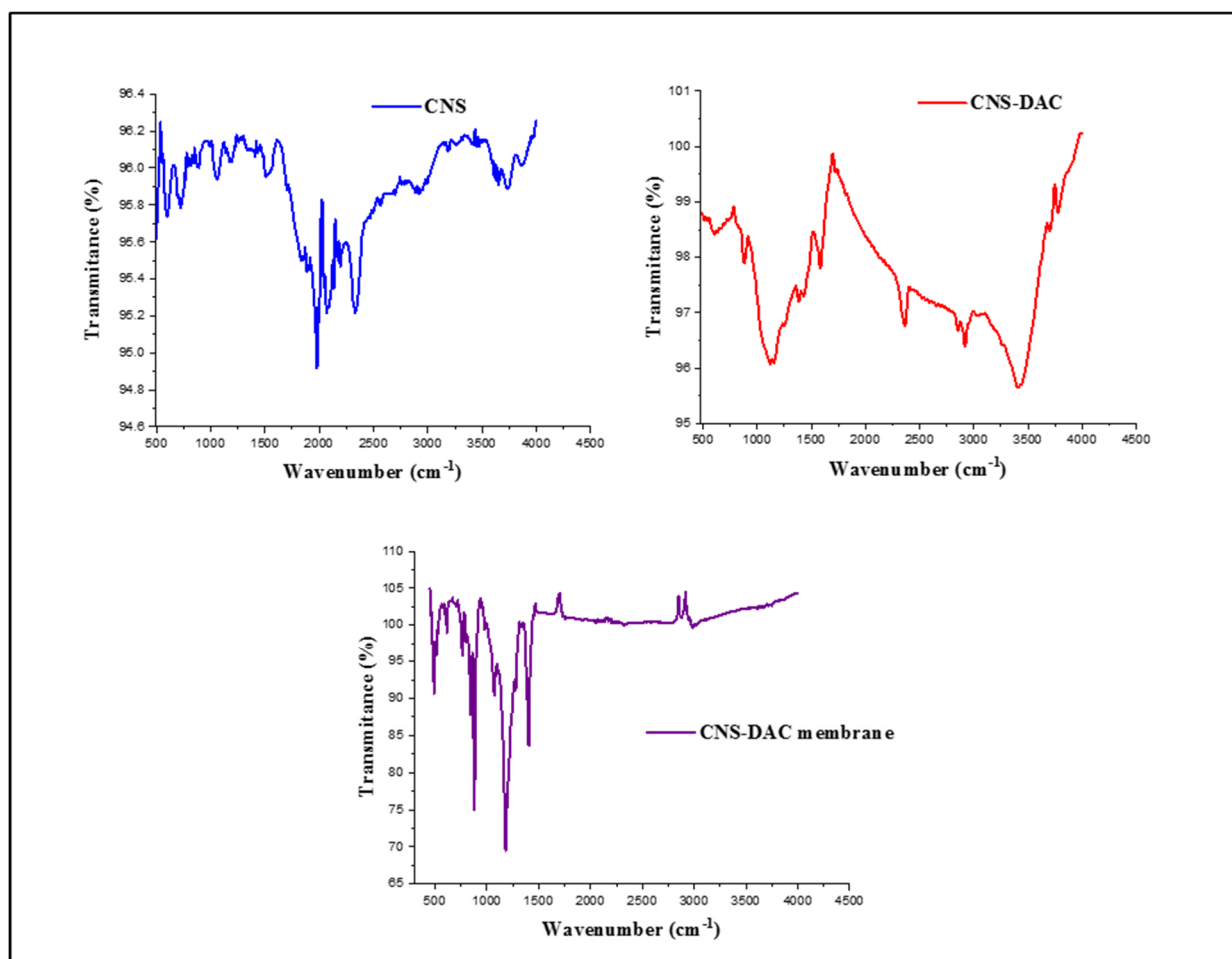


Figure 3. FTIR spectra of CNS, CNS-DAC, and a CNS-DAC membrane.

3.2.2. The Dispersion Ability of Functionalized CNSs

CNSs' spreading in the membrane's solvent and polymer matrix is one of the most crucial facets when preparing carbon nanostructures membranes or mixed-matrix membranes. It is highly recognized that using numerous types of functionalization to produce CNSs hydrophilic aims at increasing their dissolvment in aqueous solutions, particularly in organic solvents and polymer solutions.

The hydrophobic trait of CNSs, just as the solid π - π stacking connections made the CNSs simple to agglomerate or ensnare one another, is functionalization, or introducing macromolecules on the CNSs surface to facilitate their dispersion in various solutions. From Figure 4, and following one-minute sonication brought about a mix conduct of three stages: a drifting layer, sinking particles, and scattered nanospheres. It can be recognized that the modification with DAC:EG solvent revealed good dispersion compared with pristine CNSs, which is attributed to the attached hydrophilic groups on the CNSs surface. Furthermore, a good dispersion of CND-DES in the polymer is observed due to the hydrogen bonding exchanges amongst the functionalized CNSs and the polymer-solvent. Noteworthy, the increase in the solution thickness was due to the physical barrier resulted from the abate combination and decrease in the space size of polymer mixes. A membrane with a higher compatibility construction will be synthesized by higher scattering of changed CNSs in a polymer lattice, and it will additionally increase the membrane's presentation. In concurrence with past discoveries, phosphonium-based DESs were found to be less effective than ammonium-based DESs.

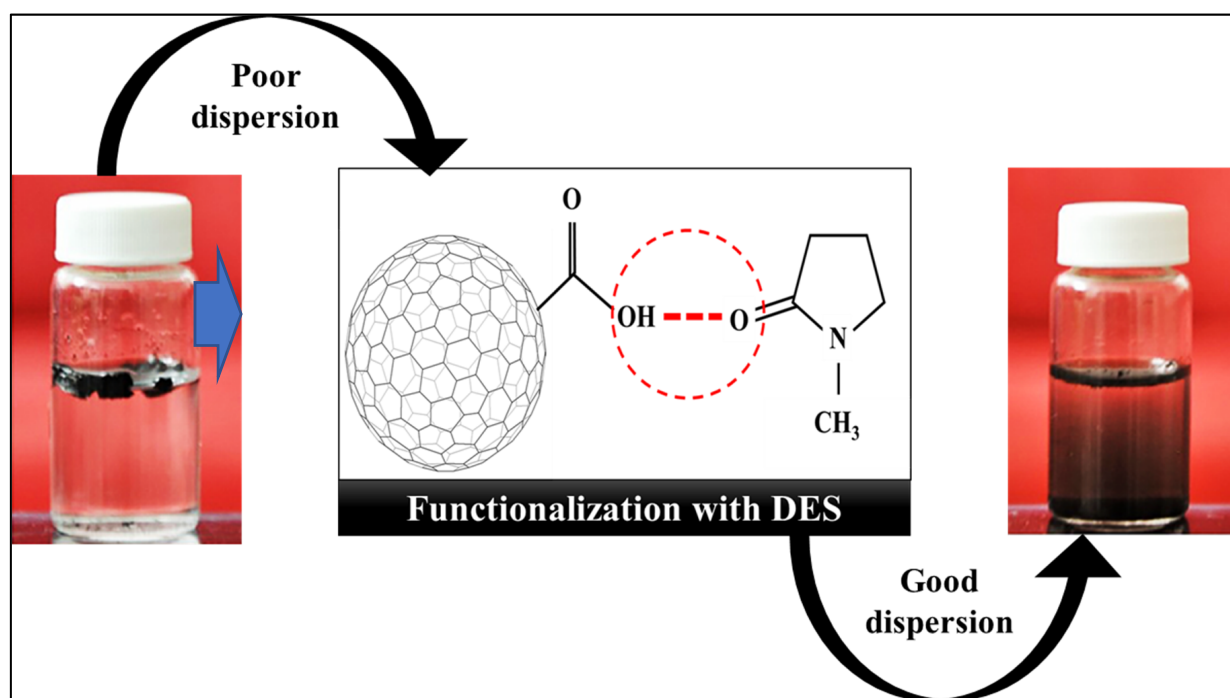


Figure 4. The effect of DESs' functional groups on the dispersion of CNS.

3.2.3. SEM, Porosity, and Thickness Analyses

SEM was employed to examine the alterations in the composite membrane morphology due to the addition of CNS. Figure 5 provides the SEM pictures for the nanocomposite membranes' cross-sections. In the latter, a typical finger-like construction was observed, which were primed from pure PVDF-HFP, whereas the addition of 1 wt.% CNS changes the cross-section whereby two layers emerge from one finger-like structure near the top surface in addition to a sponge-like structure near the bottom surface, as presented in Figure 5a. Further increases in CNS content, for example, to 3 and 5 wt.%, result in a thinner finger-like structure nearby the upper surface, while the width of the sponge layer near the bottom surface increases, as shown in Figure 5b,c. It is worth mentioning that the presence of CNS in the casting solution is a hindrance for water penetration into the casting solution through the membrane. This was the principle reason for the emergence of the sponge layer at the bottom of the membrane cross-section [29].

As CNS loading increased from 1 to 3 wt.%, membrane porosity increased from 61.92% to 68.88%, as shown in Figure 6. However, further increases in the CNSs loading, up to 5 wt.%, resulted in a severe porosity increase (up to 96.94%). This observation confirms the significant effect exerted by CNSs on the membrane porosity. The porosity expansion in the composite membranes is firmly connected to the commonness and associations of CNS control inside the polymer solution, which obstructs the NMP/water trade through the membrane, bringing about a development of a permeable design. Regarding the effects of loading the casting solution with CNS on the composite membrane thickness, it can be witnessed that the flat sheet membrane's thickness decreased from 210 to 170 μm as the CNS loading increased from 1 to 3 wt.%. However, a further increase to 5 wt.% results in a reduction of the membrane thickness to 165 μm .

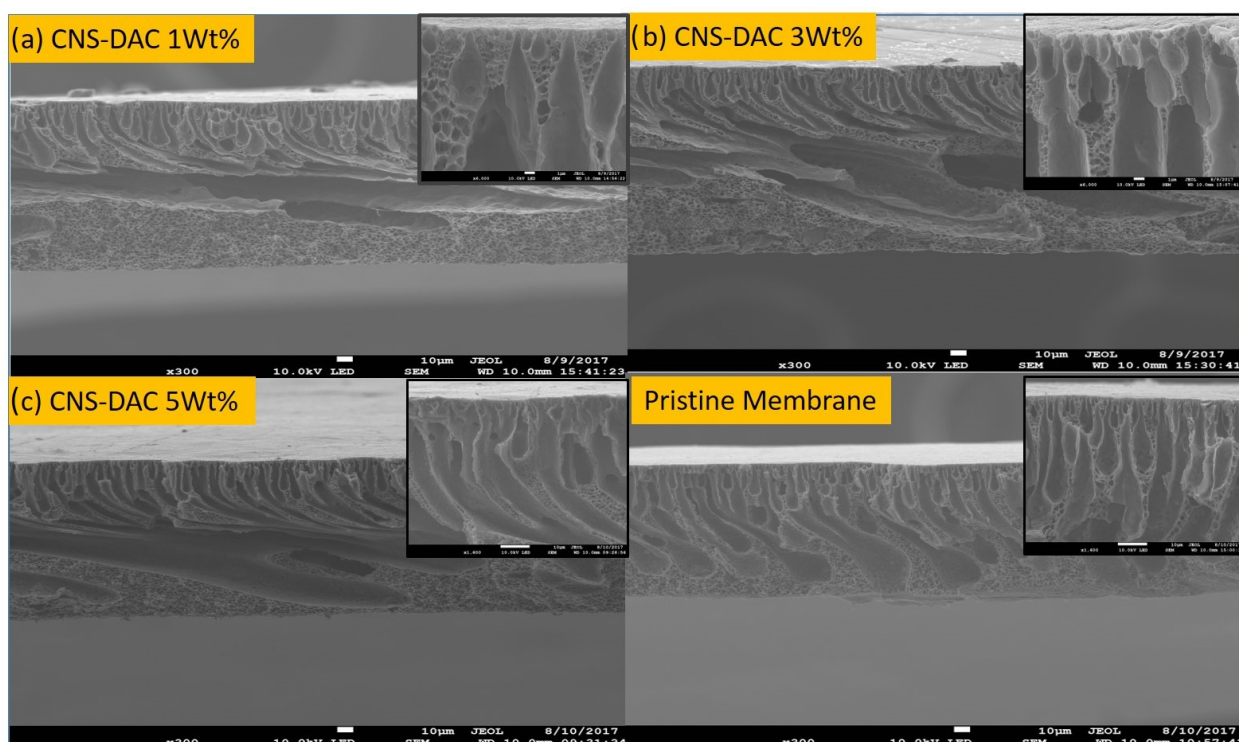


Figure 5. SEM micrographs of the composite membranes' cross-sectional area.

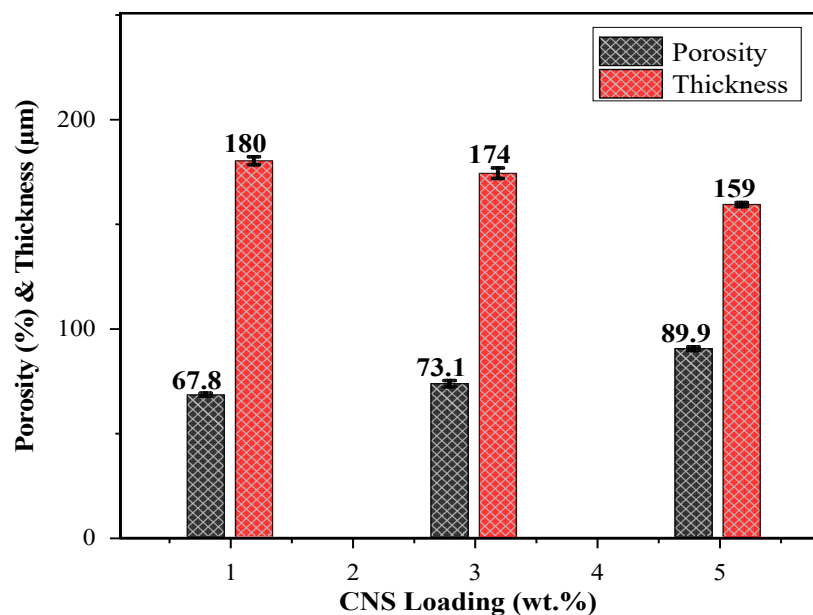


Figure 6. The effect of CNS loading in casting solution on the porosity and thickness of the composites' membrane.

3.2.4. Surface Topology and Roughness

The nodular structure is shaped on the PVDF-co-HFP/DAC-CNS membrane's top surface with interrelated hollow channels between the agglomerated knobs. The nodule size increased as the CNS loading in the polymer solution increased from 1 and 3 wt.%, whereas it decreased when 5 wt.% CNS loading was used, as shown in Figure 7. The formation of structural nodules on the membrane surface was mainly due to the modification in the diffusion's rate between NMP (solvent) and water (non-solvent) through the membrane. The upward distance between knob tops and valleys enables the estimation of

the membrane harshness, and there is an immediate connection between a membrane's performance and coarseness. Figure 8 represents the impact of CNS loading on the roughness of the PVDF-HFP/CNS membrane. Upon the augmentation of CNS loading from 1 to 3 wt.%, the membrane roughness also rises, while a reduction in the roughness is observed for 5 wt.% CNS loading; although, it is still greater than that of a membrane free from CNS. During the membrane foundation, a delay in the interchange frequency amongst solvent and non-solvent occurs, which justifies the rise accompanying the CNS loading. Later, an observed roughness reduction should be closely linked to the formation of some agglomeration and entanglement of CNS, resulting in non-homogenous distribution. It is noteworthy to point out that in the MD process high membrane roughness holds a noteworthy influence on the membrane flux.

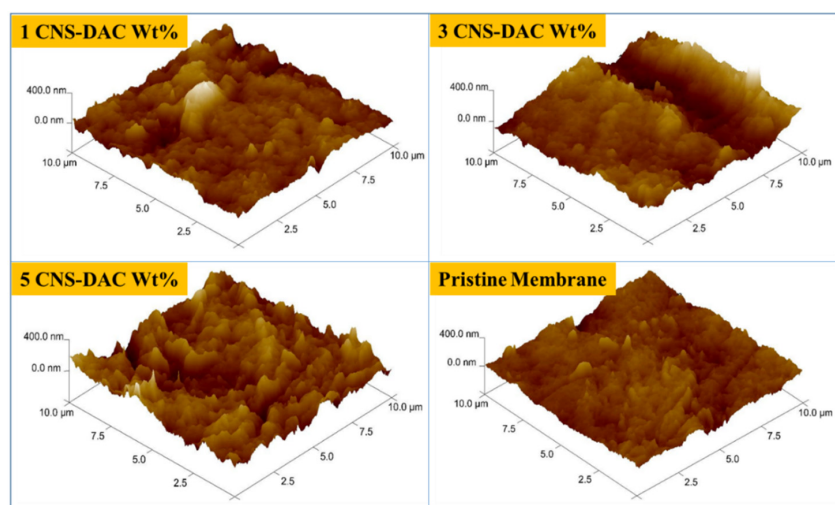


Figure 7. 3D AFM images of the membrane prepared from different CNS loadings.

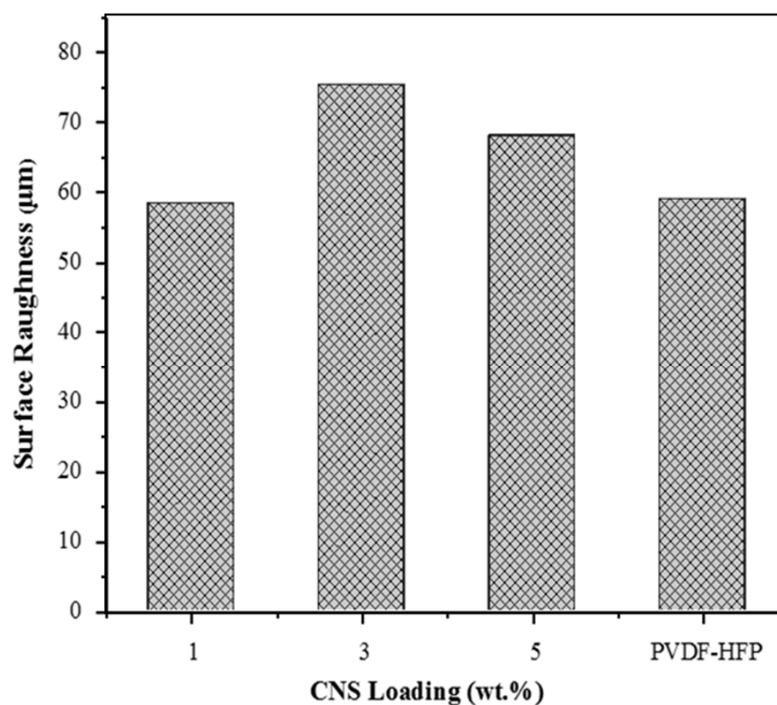


Figure 8. The CNS loading's impact in casting a solution on the roughness of the composites' membrane.

3.2.5. CA of the Nanocomposite Membrane

The contact angle (CA) is a membrane feature that reflects the ability of water to penetrate through the membrane wall. In MD processes, the membrane should be hydrophobic, such that the water vapor is solely permitted to penetrate the membrane body. For the sake of refining the membrane hydrophobicity and augmenting its performance, the hydrophobic CNSs prepared by the method described above was added to the polymer casting solution with various loadings (i.e., 1, 3, and 5 wt.%). Figure 9 presents the CAs of the membranes primed from numerous CNS loadings in the casting solution. It is illustrated that CA of PVDF-co-HFP/CNS is improved from 83° to 87° with the increase in the CNS loading to 1 wt.%. An additional rise to 3 and 5 wt.% brings about a critical expansion in the CA to 125° and 133°, respectively.

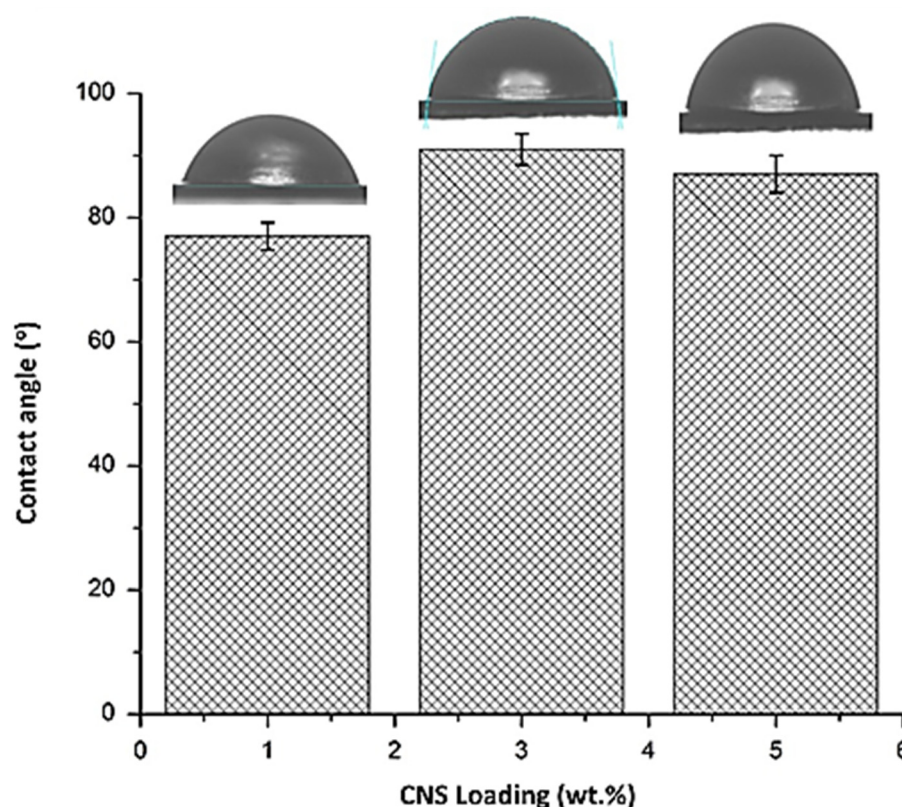


Figure 9. The CNS loading's impact in casting a solution on the contact angle of the composites' membrane.

The membrane's CA arranged from PVDF-co-HFP/CNS increases due to the significant CNS distribution across the membrane surface. Madaeni et al. clarified this peculiarity and revealed that inserting carbon nanostructures in the pores of the microfiltration PVDF membrane brought about the development of miniature- and/or nano-harshness on the PDMS-covered layer's outside surface; hence expanding the membrane harshness. This phenomenon results in air bubbles being trapped in the roughened surface and increases the hydrophobic properties [30].

3.3. Membrane Anti-Biofouling Study

In order to supervise the *S. aureus* action's conduct and the biofilm development, the CNS stacking in the membrane network has been altered after openness to various time pauses. The endured bacteria's quantity was therefore evaluated by plating and including of OD in a flagon.

Table 1 and Figure 10 represent the number of survival cells compared to the exposure time for the composite membranes. There was no detection of antibacterial motion in the

pure PVDF-HFP membrane. In contrast, great evidence was obtained indicating that the assimilated CNS to the PVDF-HFP membrane inhibited the number of bacteria cells and imparted antibacterial activity to the membrane. It is reported that high hydrophobicity could help control biofouling and that the rough surface was responsible for the reduction of bacterial attachment to the surface of membranes. Hydrophobicity decreased the contact area between the membrane surface and water; thus minimizing the chance of biofouling reaching the surface. The bacterial growth of *S. aureus* was accumulated on PVD-HFP, which can lead to irreversible adhesion of membrane biofouling. However, after adding the CNS, the accumulation was less dependent on the amount of CNS. The prepared novel hybrid membrane (PVDF-co-HFP/CNS) exhibited higher anti-biofouling characteristics than the pure PVDF-HFP membrane after loading a high amount of CNS, as shown in Figure 11.

Table 1. The survival cells' quantity compared to the exposure time for the composite membranes.

Samples	24 h ($\times 10^8$ CFU)	48 h ($\times 10^8$ CFU)	73 h ($\times 10^8$ CFU)	120 h ($\times 10^8$ CFU)
PVDF-HFP	0.90 ± 0.068 b	1.38 ± 0.051 b	1.38 ± 0.6418 e	1.29 ± 0.115 b
1 CNS-DAC wt.%	0.79 ± 0.036 c	1.007 ± 0.0912 d	1.114 ± 0.04684 b	0.98 ± 0.047 c
3 CNS-DAC wt.%	0.94 ± 0.063 e	1.23 ± 0.047 b	1.29 ± 0.042 b	1.09 ± 0.393 e
5 CNS-DAC wt.%	0.97 ± 0.043 a	1.18 ± 0.036 e	1.32 ± 0.035 c	1.21 ± 0.153 a

Note: CFU = colony-forming units of bacteria per millilitre (CFU/mL); \pm shows the values are the mean of five replicates experiments. The values represent the mean of five replicates, where the different letter(s) in each column represents a significant difference ($p < 0.05$) calculated through the dmrt test.

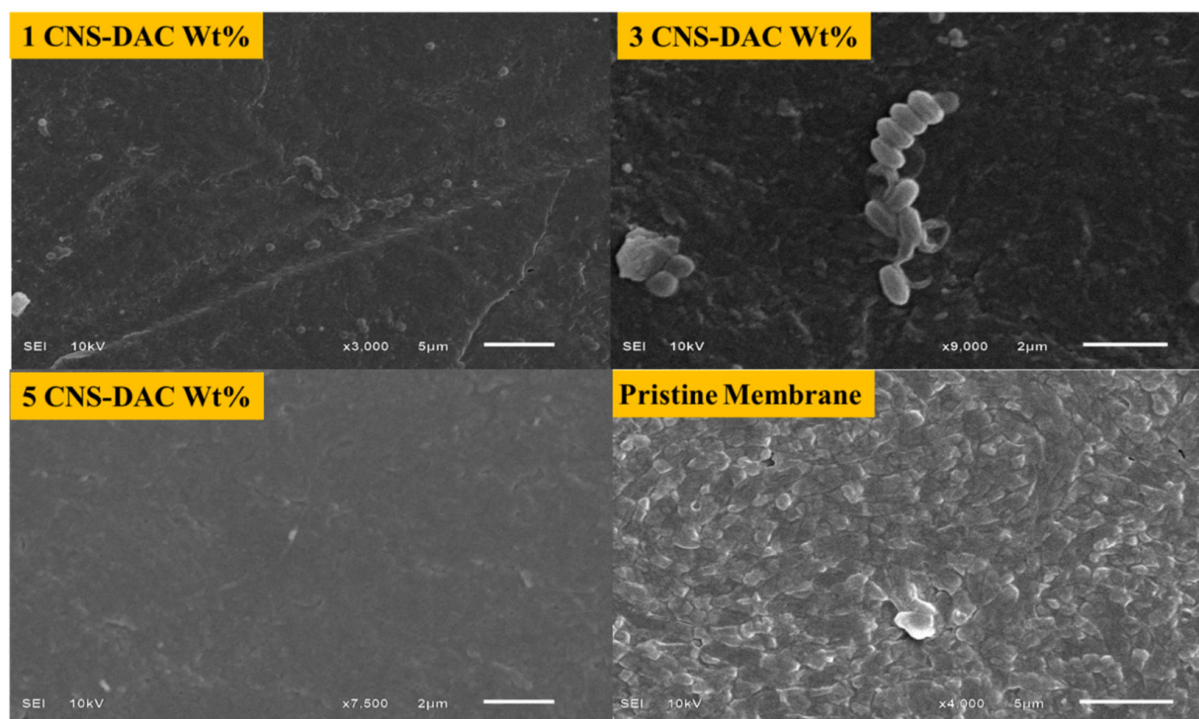


Figure 10. Bacterial adhesion and growth on the pristine membrane, the CNS-DAC membrane at different CNS loading (wt.%) for a period of up to 120 h.

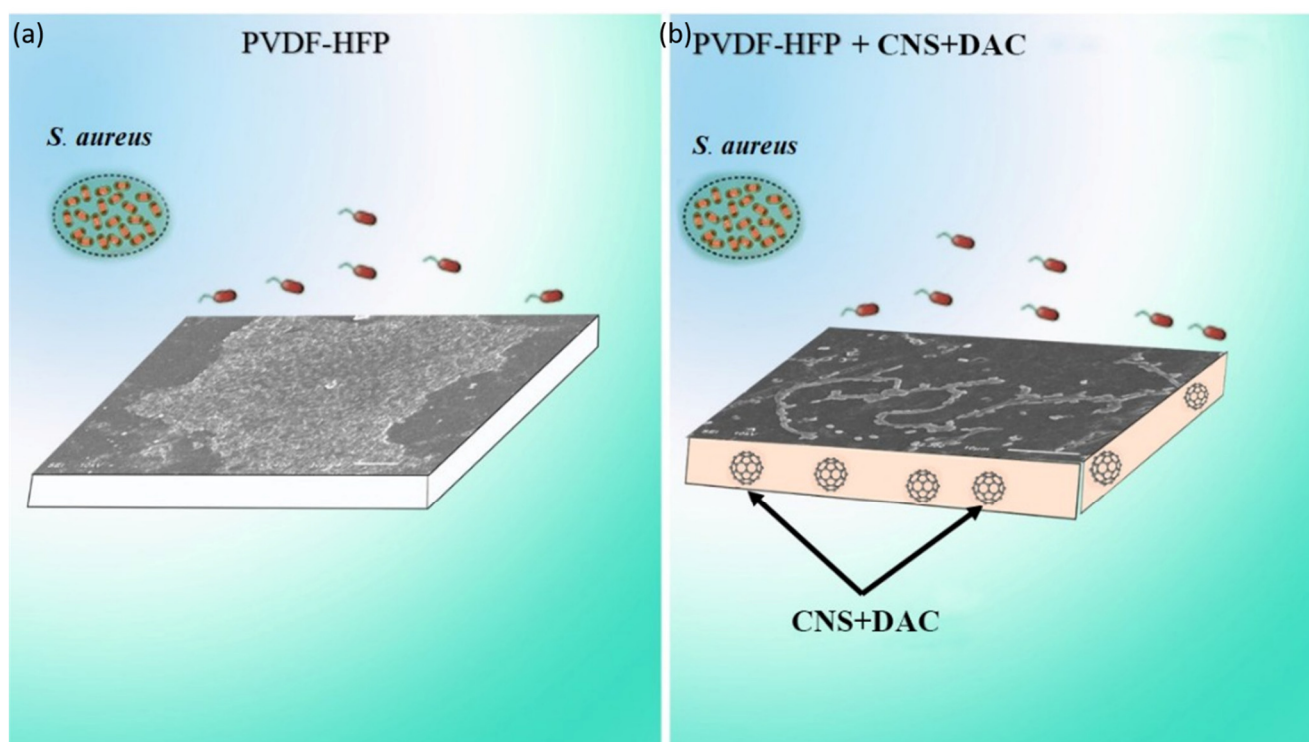


Figure 11. Bacterial adhesion on (a) the pristine membrane and (b) the CNS-DAC membrane.

3.4. DCMD Performance

Figure 11 shows the verification of 1, 3, and 5 wt.% nanocomposite membranes' performance, which was conducted in a DCMD arrangement framework. Moreover, the composite membranes' performance was developed by CNS with regard to distillation through the creation of high saturation flux. The permeation flux of PVDF-co-HFP/CNS composite membrane increased as the CNS loading increased. The average salt rejection of all membranes remained >99.9% throughout the duration of the experiment. These results show that modification of PVDF-HFP by DES modified CNS particles can improve the membrane performance for DCMD, as the permeation flux was increased from 10 for pure PVDF-co-HFP membrane to 35 L/h/m² for the membrane with 5 wt.% of CNS. This phenomenon is accredited to the rise in membrane porosity and CA, along with decreasing membrane thickness, as a result of increasing CNS loading. Relying on the study's achieved outcomes, it is possible to draw the conclusion that the CNS-DAC offers promising opportunities when incorporated into the PVDF-HFP solution. Additionally, incorporating CNS-DAC in the membrane body resulted in high membrane flux size and surface area, which can favor the reciprocal action of vapor molecules with CNS, permitting their movement from the feed side to the permeated side by a surface/intra-particle dispersion process, in agreement with previous studies [31]. In comparison with previous work [11], where the membrane was prepared from a mixture comprising of 12 wt.% PVDF-HFP and isopropanol solution as a coagulation bath, it can be noticed that using a lower feed temperature of 45 °C in this study, a similar permeation flux of 16 L/h/m² was attained to that when 60 °C was used in the previous work [38]. This outcome is due to the higher porosity, lower thickness, and higher CA of the hierarchical PVDF-HFP membrane, which was arranged employing the method described in this work. Additionally, the prepared PVDF-co-HFP/DAC-CNS membrane with 5 wt.% CNS was evaluated for its potential to purify the dye wastewater containing MO, with a dye concentration of 50 ppm. The purification performance of the prepared membrane is visualized in Figure 12. The synthesized hierarchical membrane rejected 99.9% of methyl orange, demonstrating a great performance. According to the results, the surface negative charge of the PVDF-co-HFP/DAC-CNS membrane increased by incorporating DAC-CNS. Thus, the rejection of MO is because of a charge repulsion

among the membrane surface and anionic dye leading to a weaker adsorption of the dye molecules on the membrane surface and higher water penetration. Furthermore, a notable high rejection effect can be obtained with a higher molecular weight dye due to the size exclusion hindrance. Consequently, the preparation method introduced in the current research, namely the accessibility of DAC-CNS, and multifunctional presentation (water flux and refusal), validate this kind of membrane's efficiency for dye remediation. Accordingly, charge repulsion holds responsible for the anionic MO dye is rejected, which results in the compounds' lower adsorption on the membrane surface and higher water saturation. Furthermore, a substantial high rejection effect can be obtained with a higher molecular weight dye by ideals of more steric impediment and electrostatic repugnance impacts. Taking into account the previously mentioned clarifications, the creation strategy utilized in this research, namely the accessibility of DAC-CNS and viable execution (water transition and dismissal), show this kind of membranes' capability in the expulsion of color from water.

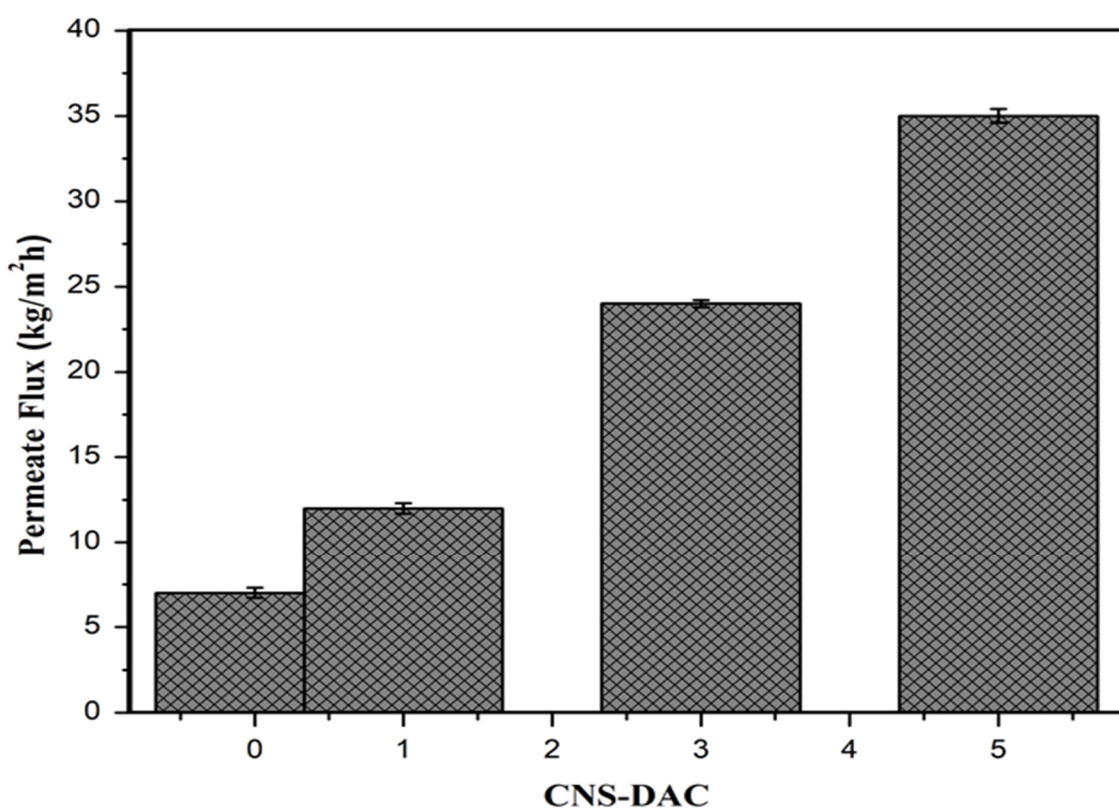


Figure 12. The effect of CNS loading on a permeate flux and MO removal.

4. Conclusions

In the current work, different contents of carbon nanospheres, which were modified with deep eutectic solvent, were incorporated in the poly(vinylidene fluoride-co-hexafluoropropylene) (PVDF-co-HFP) membrane matrix. The pre-arranged membranes were portrayed by morphological and performance qualities. The modified CNS content enjoys a significant part in the morphological structure as well as the membrane's hydrophobic character. The CNS confinement yielded a substantial increase in its hydrophobicity and porosity, alongside a reduction in membrane thickness. Moreover, there was an augmentation of DCMD saturation through the hierarchal membrane from 12 to 35 L/m²/h by implanting 5 wt.% of CNSs at the feed temperature of 45 °C with salt dismissal >99.9%. Furthermore, the hybrid membrane's performance was assessed with regard to the elimination of methyl orange dye from water. The prepared membrane presented supreme efficiency in dye rejection from the water with a concentration of 50 ppm. This work established that the investigated approach in the presented research can well

challenge the commercial membranes when it comes to the adequate permeability, high dye elimination, as well as green nano-additive utilization.

Author Contributions: Conceptualization, Q.F.A., M.M.H. and M.M.A.; methodology, M.M.A., H.S.M. and M.A.A.; software, H.M.A. and M.A. validation, Q.F.A., M.M.A. and N.S.A.; formal analysis, M.M.H. and B.I.; investigation, Q.F.A., M.M.A. and M.A.A.; writing—original draft preparation, Q.F.A., N.S.A., A.E.M. and H.M.A.; writing—review and editing, Q.F.A. and Z.B.M.; supervision, Q.F.A. and M.M.A. All authors have read and agreed to the published version of the manuscript.

Funding: This research received no external funding.

Data Availability Statement: Not applicable.

Conflicts of Interest: The authors declare no conflict of interest.

References

- Alayan, H.M.; Aljumaily, M.M.; Alsaadi, M.A.; Mjalli, F.S.; Hashim, M.A. A review exploring the adsorptive removal of organic micropollutants on tailored hierarchical carbon nanotubes. *Toxicol. Environ. Chem.* **2021**, 1–61, just-accepted.
- Alayan, H.M.; Hussain, I.R.; Kamil, F.H.; Aljumaily, M.M.; Hashim, N.A. Proficiency of Few-Layered Graphene Oxide Nanosheets as Promising Sorbents for Dye Pollution Management. *J. Environ. Eng.* **2020**, *146*, 04020090. [[CrossRef](#)]
- Alayan, H.M.; Alsaadi, M.A.; Abo-Hamad, A.; AlOmar, M.K.; Aljumaily, M.M.; Das, R.; Hashim, M.A. Hybridizing carbon nanomaterial with powder activated carbon for an efficient removal of Bisphenol A from water: The optimum growth and adsorption conditions. *Desalination Water Treat.* **2017**, *95*, 128–143.
- AlOmar, M.K.; Alsaadi, M.A.; Aljumaily, M.M.; Akib, S.; Jassam, T.M.; Hashim, M.A. N,N-diethylethanolammonium chloride based DES-functionalized carbon nanotubes for arsenic removal from aqueous solution. *Desalination Water Treat.* **2017**, *74*, 163–173. [[CrossRef](#)]
- Aljumaily, M.M.; Alsaadi, M.A.; Hashim, N.A.; Alsally, Q.F.; Mjalli, F.S.; Atieh, M.; Al-Harrasi, A. PVDF-co-HFP/superhydrophobic acetylene-based nanocarbon hybrid membrane for seawater desalination via DCMD. *Chem. Eng. Res. Des.* **2018**, *138*, 248–259. [[CrossRef](#)]
- Ibrahim, R.K.; El-Shafie, A.; Hin, L.S.; Mohd, N.S.B.; Aljumaily, M.M.; Ibraim, S.; AlSaadi, M.A. A clean approach for functionalized carbon nanotubes by deep eutectic solvents and their performance in the adsorption of methyl orange from aqueous solution. *J. Environ. Manag.* **2019**, *235*, 521–534. [[CrossRef](#)]
- Küçükosmanoğlu, M.; Gezici, O.; Ayar, A. The adsorption behaviors of Methylene Blue and Methyl Orange in a diaminoethane sporopollenin-mediated column system. *Sep. Purif. Technol.* **2006**, *52*, 280–287. [[CrossRef](#)]
- Vandevivere, P.C.; Bianchi, R.; Verstraete, W. Review: Treatment and reuse of wastewater from the textile wet-processing industry: Review of emerging technologies. *J. Chem. Technol. Biotechnol.* **1998**, *72*, 289–302. [[CrossRef](#)]
- Mohan, S.V.; Rao, N.C.; Karthikeyan, J. Adsorptive removal of direct azo dye from aqueous phase onto coal based sorbents: A kinetic and mechanistic study. *J. Hazard. Mater.* **2002**, *90*, 189–204. [[CrossRef](#)]
- Aljumaily, M.M.; Alsaadi, M.A.; Hashim, N.A.B.; Mjalli, F.S.; Alsally, Q.F.; Khan, A.L.; Al-Harrasi, A. Superhydrophobic nanocarbon-based membrane with antibacterial characteristics. *Biotechnol. Prog.* **2020**, *36*, e2963. [[CrossRef](#)]
- Alanezi, A.A.; Alanezi, Y.A.; Alazmi, R.; Altaee, A.; Alsally, Q.F.; Sharif, A.O. Enhancing performance of the membrane distillation process using air injection zigzag system for water desalination. *Desalination Water Treat.* **2020**, *207*, 43–50. [[CrossRef](#)]
- Aljumaily, M.M.; Alsaadi, M.A.; Das, R.; Hamid, S.B.A.; Hashim, N.A.; AlOmar, M.; Alayan, H.; Novikov, M.; Alsally, Q.F.; Hashim, M.A. Optimization of the Synthesis of Superhydrophobic Carbon Nanomaterials by Chemical Vapor Deposition. *Sci. Rep.* **2018**, *8*, 2778. [[CrossRef](#)]
- Jamed, M.J.; Alanezi, A.A.; Alsally, Q.F. Effects of embedding functionalized multi-walled carbon nanotubes and alumina on the direct contact poly(vinylidene fluoride-co-hexafluoropropylene) membrane distillation performance. *Chem. Eng. Commun.* **2018**, *206*, 1035–1057. [[CrossRef](#)]
- Mulder, J. *Basic Principles of Membrane Technology*; Springer Science & Business Media: Berlin/Heidelberg, Germany, 2012.
- Dumée, L.F.; Sears, K.; Schutz, J.; Finn, N.; Huynh, C.; Hawkins, S.; Duke, M.; Gray, S. Characterization and evaluation of carbon nanotube Bucky-Paper membranes for direct contact membrane distillation. *J. Membr. Sci.* **2010**, *351*, 36–43. [[CrossRef](#)]
- Yin, J.; Deng, B. Polymer-matrix nanocomposite membranes for water treatment. *J. Membr. Sci.* **2015**, *479*, 256–275. [[CrossRef](#)]
- Fadhil, S.; Marino, T.; Makki, H.F.; Alsally, Q.F.; Blefari, S.; Macedonio, F.; Di Nicolò, E.; Giorno, L.; Drioli, E.; Figoli, A. Novel PVDF-HFP flat sheet membranes prepared by triethyl phosphate (TEP) solvent for direct contact membrane distillation. *Chem. Eng. Process. Process Intensif.* **2016**, *102*, 16–26. [[CrossRef](#)]
- Das, R.; Ali, E.; Hamid, S.B.A.; Ramakrishna, S.; Chowdhury, Z. Carbon nanotube membranes for water purification: A bright future in water desalination. *Desalination* **2014**, *336*, 97–109. [[CrossRef](#)]
- Das, R.; Hamid, S.B.A.; Ali, M.E.; Ismail, A.F.; Annuar, M.S.M.; Ramakrishna, S. Multifunctional carbon nanotubes in water treatment: The present, past and future. *Desalination* **2014**, *354*, 160–179. [[CrossRef](#)]

20. Tittmann-Otto, J.; Hermann, S.; Kalbacova, J. Effect of cleaning procedures on the electrical properties of carbon nanotube transistors—A statistical study. *J. Appl. Phys.* **2016**, *119*, 124509. [\[CrossRef\]](#)
21. Hayyan, M.; Hashim, M.A.; Al-Saadi, M.A.; Hayyan, A.; AlNashef, I.M.; Mirghani, M.E. Assessment of cytotoxicity and toxicity for phosphonium-based deep eutectic solvents. *Chemosphere* **2013**, *93*, 455–459. [\[CrossRef\]](#)
22. Hayyan, A.; Mjalli, F.S.; AlNashef, I.; Al-Wahaibi, T.; Al-Wahaibi, Y.; Hashim, M.A. Fruit sugar-based deep eutectic solvents and their physical properties. *Thermochim. Acta* **2012**, *541*, 70–75. [\[CrossRef\]](#)
23. Yang, D.; Hou, M.; Ning, H.; Zhang, J.; Ma, J.; Yang, G.; Han, B. Efficient SO₂ absorption by renewable choline chloride–glycerol deep eutectic solvents. *Green Chem.* **2013**, *15*, 2261–2265. [\[CrossRef\]](#)
24. Li, X.; Hou, M.; Han, B.; Wang, X.; Zou, L. Solubility of CO₂ in a Choline Chloride + Urea Eutectic Mixture. *J. Chem. Eng. Data* **2008**, *53*, 548–550. [\[CrossRef\]](#)
25. Carriazo, D.; Serrano, M.C.; Gutiérrez, M.C.; Ferrer, M.L.; del Monte, F. Deep-eutectic solvents playing multiple roles in the synthesis of polymers and related materials. *Chem. Soc. Rev.* **2012**, *41*, 4996–5014. [\[CrossRef\]](#)
26. Mamun, A.; Ahmed, Y.M.; Muyibi, S.; Al-Khatib, M.; Jameel, A.; Alsaadi, M. Synthesis of carbon nanofibers on impregnated powdered activated carbon as cheap substrate. *Arab. J. Chem.* **2016**, *9*, 532–536. [\[CrossRef\]](#)
27. Alsally, Q.F.; Ali, J.M.; Abbas, A.A.; Rashed, A.; Van Der Bruggen, B.; Balta, S. Enhancement of poly(phenyl sulfone) membranes with ZnO nanoparticles. *Desalination Water Treat.* **2013**, *51*, 6070–6081. [\[CrossRef\]](#)
28. Alsally, Q.F.; Rashid, K.T.; Ibrahim, S.S.; Ghanim, A.H.; Van der Bruggen, B.; Luis, P.; Zablouk, M. Poly (vinylidene fluoride-co-hexafluoropropylene)(PVDF-co-HFP) hollow fiber membranes prepared from PVDF-co-HFP/PEG-600Mw/DMAC solution for membrane distillation. *J. Appl. Polym. Sci.* **2013**, *129*, 3304–3313. [\[CrossRef\]](#)
29. Silva, T.L.S.; Morales-Torres, S.; Figueiredo, J.; Silva, A. Multi-walled carbon nanotube/PVDF blended membranes with sponge- and finger-like pores for direct contact membrane distillation. *Desalination* **2015**, *357*, 233–245. [\[CrossRef\]](#)
30. Chung, Y.T.; Mahmoudi, E.; Mohammad, A.W.; Benamor, A.; Johnson, D.; Hilal, N. Development of polysulfone-nanohybrid membranes using ZnO-GO composite for enhanced antifouling and antibacterial control. *Desalination* **2017**, *402*, 123–132. [\[CrossRef\]](#)
31. Machado, F.M.; Bergmann, C.P.; Fernandes, T.H.; Lima, E.C.; Royer, B.; Calvete, T.; Fagan, S.B. Adsorption of Reactive Red M-2BE dye from water solutions by multi-walled carbon nanotubes and activated carbon. *J. Hazard. Mater.* **2011**, *192*, 1122–1131. [\[CrossRef\]](#)
32. Coates, J. Interpretation of infrared spectra, a practical approach. In *Encyclopedia of Analytical Chemistry*; John Wiley & Sons Ltd.: Chichester, UK, 2000; pp. 10815–10837.
33. Das, A.K.; Maiti, S.; Khatua, B. High performance electrode material prepared through in-situ polymerization of aniline in the presence of zinc acetate and graphene nanoplatelets for supercapacitor application. *J. Electroanal. Chem.* **2015**, *739*, 10–19. [\[CrossRef\]](#)
34. Maiti, S.; Khatua, B.B. Electrochemical and electrical performances of cobalt chloride (CoCl₂) doped polyaniline (PANI)/graphene nanoplate (GNP) composite. *RSC Adv.* **2013**, *3*, 12874–12885. [\[CrossRef\]](#)
35. Sheng, G.; Shao, D.; Ren, X.; Wang, X.; Li, J.; Chen, Y. Kinetics and thermodynamics of adsorption of ionizable aromatic compounds from aqueous solutions by as-prepared and oxidized multiwalled carbon nanotubes. *J. Hazard. Mater.* **2010**, *178*, 505–516. [\[CrossRef\]](#) [\[PubMed\]](#)
36. Stuart, B.H. *Infrared Spectroscopy: Fundamentals and Applications*/H. Barbara Stuart; Wiley: Hoboken, NJ, USA, 2004; 224p.
37. AlOmar, M.; Alsaadi, M.A.; Hayyan, M.; Akib, S.; Ibrahim, R.K.; Hashim, M.A. Lead removal from water by choline chloride based deep eutectic solvents functionalized carbon nanotubes. *J. Mol. Liq.* **2016**, *222*, 883–894. [\[CrossRef\]](#)
38. Aljumaily, M.M.; Alsaadi, M.A.; Awanis Hashim, N.; Alsally, Q.F.; Das, R.; Mjalli, F. Embedded high-hydrophobic CNMs prepared by CVD technique with PVDF-co-HFP membrane for application in water desalination by DCMD. *Desalination Water Treat.* **2019**, *142*, 37–48. [\[CrossRef\]](#)